# Small Wind Turbine Control with Detection of Grid Failure Operating in Both Grid and Stand-Alone

[1]Nikam Sudhir Kanhaiyalal, [2]Prof. N.L.Potdar

Department of Electrial Engg.
(K.K.Wagh, Nasik)

***Abstract*: For variable speed grid connected wind energy generation system a new control scheme is presented. A back-to-back power converter capable of working in both stand-alone and grid-connection mode, the development and test of a flexible control strategy for an 11-kW wind turbine is with back-to-back power converter.**

**The design of a phase-locked loop (PLL) is described for the power factor control of grid-connected three-phase power conversion systems as well as detection of failure in Grid. Also PLL is worked as a switching purpose between Stand-Alone and Grid-Connected mode accordingly.**

**Development of user-friendly code and online tuning is used to implement and test the different control strategies by a flexible digital signal processor (DSP) system.**

***Keywords*: Digital signal processor (DSP) control, grid failure, phase-locked loop (PLL), wind turbine (WT).**

## I. INTRODUCTION

The range of 11 kW Small efficient wind turbines (WT) in as depicted in Fig. 1 can be used to supply farms or private houses in faraway locations in developing countries where low-cost access to the electrical power grid is impractical. Squirrel cage Induction motors are the most commonly used electrical machine in AC drives, because they are cheap, robust and have low maintenance cost. These advantages make the induction machine very attractive for wind power applications both for fixed As well as variable speed operation. To take advantage of the higher energy capture and increase in the system compliance resulting from variable speed operation a power electronic interface must be provided between the machine terminals and the grid. The back-to-back PWM inverter based power electronics interface is a suitable option for cage induction machine in wind power applications. But some new challenges on the control side of these WT occurred like reasonable voltage regulation in stand-alone mode with nonlinear load, grid-connection mode enabled, and automatic detection of grid failure. But in order to achieve these goals, relative complex control strategies need to be developed. Also automatic mode switching and grid failure detection are required.

One stage pulse width-modulation (PWM) ac–ac power conversion faces many challenges with the unavailability of semiconductor bi-directional power switches utilizing a cost-effective design. Mostly reported ac–ac power converters [1], [2], [3] based on technology of modern semiconductor device use discrete two-quadrant devices.

The PLL technique has been used as a common way of recovering the frequency and phase information in electrical systems [4, 5]. In power electronics area, the PLL technique has been adopted for the speed control of electric motors [6, 7]. This is also available for generating the current references synchronized with the utility voltages in the power conversion system. A simple method of obtaining the phase information is to detect the zero crossing points of the utility voltages [4]. However, since the zero crossing points can be detected only at every half-cycle of the utility, the phase tracking action is impossible between the detecting points, and fast tracking performance cannot be achieved. Another method is the technique using the quadrature of the input waveform shifted by 90 degrees [4].

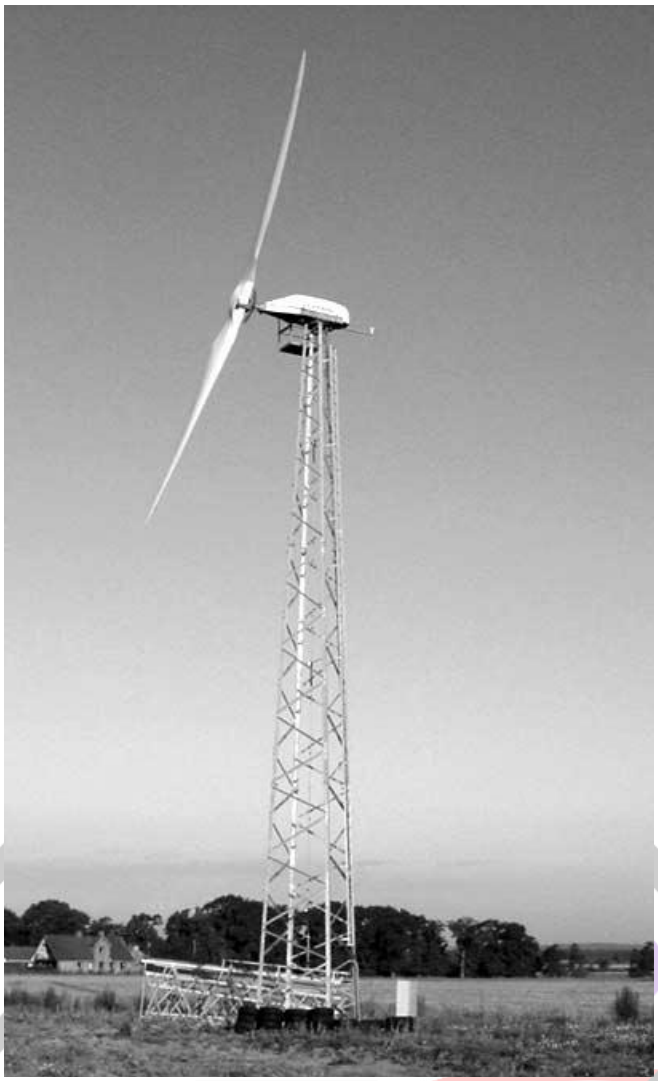

Fig. 1. Small 11-kW wind turbine

## II. STAND-ALONE WIND TURBINES

The mostly used configurations of power converters for stand-alone squirrel-cage induction generators (SCIG) wind turbine (WT) are shown in Fig. 2.

The Fig. 2(a) shows diode rectifier topology it can only be used in one quadrant, it is simple and not possible to control it. This configuration is especially suitable for constant speed wind turbines and requires a capacitor bank between the generator and the diode rectifier in order to magnetize the induction generator.

The back-to-back voltage source converter is a two way directional power converter existing of two conventional voltage sources can be obtained by properly connecting the output terminals of the converter to the input terminals. Some advantages of the matrix converters are less thermal stress of the semiconductors for a low output frequency compared with the back-to-back solution and the absence of the dc-link capacitor that may increase the efficiency and the lifetime. As drawbacks can be mentioned,

the intrinsic limitation of the output voltage, the unavailability of a true bi-directional switch and there is no decoupling between the input and the output of the converter as for the case of back-to-back converter and this may lead to some instability issues.

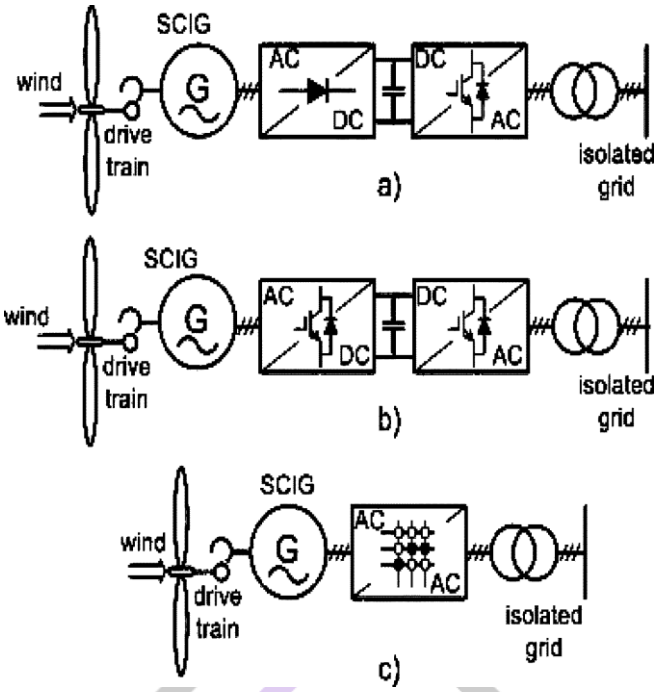


Fig. 2. Stand-alone wind turbine configurations with squirrel-cage induction generators: (a) diode bridge rectifier and voltage source inverter, (b) back-to-back voltage source converter, and (c) matrix converter.

From overall discussion on different power converter technologies that can be used in wind turbine applications [8] result is that the back-to-back converter is the less troublesome configuration mainly because it can use commercial converters at the generator side.

## III. EXPERIMENTAL SYSTEM

The system includes of two back-to-back PWM voltage fed inverters connected between a 2.5kW**,** 1450 rpm Squirrel-Cage Induction Generator (CIG) and the grid. The supply voltage has been set to 250V via a three phase variac. The DC link voltage is regulated at 550V providing enough modulation index excursion during transients to avoid over modulation problems. Three 12mH filter inductances are connected between the grid and the supply side converter. The switching frequency of the PWM converters is lk Hz, the position is measured with a 10000 ppr. encoder. The sampling time of the current, voltages and position, as well as the voltage and current control loops is set to 0.5ms unless specified otherwise. Fig. 3 shows a schematic of the system. The generator is driven by a four-quadrant DC drive emulating a wind turbine. For a given wind velocity and rotational speed a signal representing the wind turbine torque is obtained using a look up table of the wind turbine aerodynamics characteristics. This signal together with the electrical torque is used to generate a reference speed signal for the DC drive, emulating a 3.2 kW wind turbine with given inertia and fiction coefficient **[**9, 10**].** The entire system is controlled using a microprocessor network [11].

## IV. INDUCTION MACHINE CONTROL AND WIND TURBINE OPTIMUM SPEED TRACKTNG.

The SCIG currents are controlled using a standard indirect vector control, with the current and voltages referred to a d-q synchronous frame aligned with the rotor flux vector**.** The flux and the electrical torque**,** are given by:

$$\lambda_{dr} = L_o i_{mrd} = \frac{L_o i_{sd}}{1 + T_r s}$$
$$T_e = k_1 \frac{p}{2} \frac{L_o^2}{L_r} i_{mrd} i_{qs} \qquad (1)$$

Where k1 depends on the transformation used and ***isd , isq, imrd*** are the d-q axis current and the magnetising current respectively. ***Lo, Lr,*** and *T,* are the magnetising and stator self-inductances and the rotor time constant respectively. High bandwidth current control for the d-q stator component currents is achieved with the vector control approach. For below rated wind velocity, the mechanical power, ***Pm,*** of a fixed-pitch wind turbine is a function of the effective wind velocity trough the blades ***v***, the air density ***p,*** the blades radius ***R*** and the power coefficient Cp. And is given by:

$$P_m = 0.5\rho C_p(\lambda)R^2v^3 \quad (2)$$

Considering the rotational speed of the wind turbine ***o*** and the torque coefficient C, , the analytical expressions for the wind turbine mechanical torque is given by,

$$T_m = 0.5\rho C_t(\lambda)R^3v^2$$
$$C_p(\lambda) = \lambda C_t(\lambda) \quad (3)$$

**Where λ is the tip speed ratio defined by:**

$$\lambda = \frac{\omega R}{v} \quad (4)$$

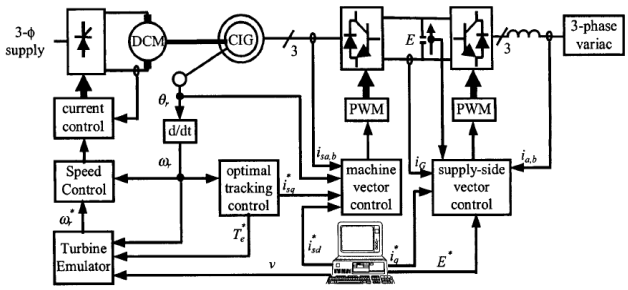


Fig. 3. Experimental Setup

## (A) TURBINE EMULATOR

The wind speed is calculated as an average value of the fixed-point wind speed over the whole rotor, and it takes the tower shadow and the rotational turbulences into account. The wind turbine mechanical shaft is emulated using a standard six-pole 15-kW/400-V squirrel-cage induction motor controlled by a commercial frequency inverter operated in open-loop torque control mode. The aerodynamic model of the wind turbine rotor is based the curve CQ – λ as shown in Fig. 4.

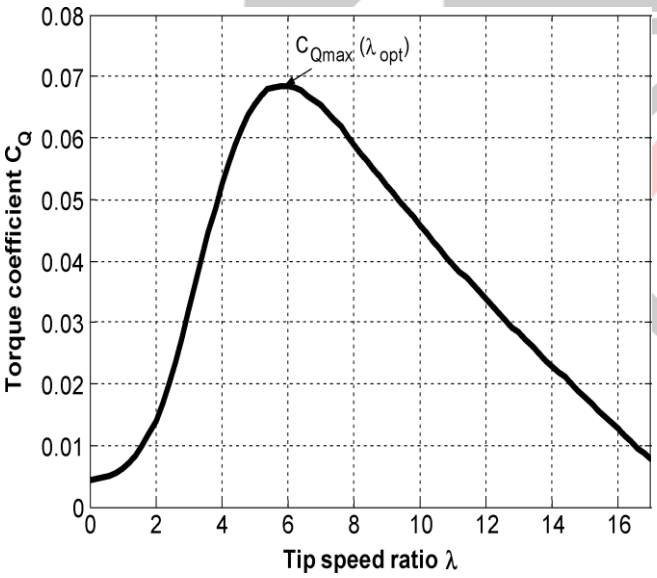


Fig. 4. CQ – λ performance curve for the wind turbine. C is the torque coefficient.

The wind turbine emulator uses a scalar open-loop torque controlled induction motor where the torque reference is chosen to be

$$\lambda^* = T_{\max,\Omega=\Omega_{opt}} \quad (5)$$

in order to extract the maximum power from the wind turbine at a given wind speed.

### (B) PWM INVERTER

The PWM inverter is operated in current-controlled mode when it is connected to the utility, and regulates the current injected into the point of common coupling. The utility is considered to be relatively stiff and maintains the voltage across the load. In the stand-alone mode, the PWM inverter is operated in the voltage-controlled mode. The inverter is controlled to regulate the voltage across the load. Thus, the PWM inverter has to be capable of shifting between current-controlled and voltage-controlled modes, to maintain the voltage across the load in the presence of faults on the grid.

The control algorithm required to transfer between the current-controlled mode and the voltage-controlled mode, should ensure that the static transfer switch turns off before the inverter shifts to the voltage-controlled mode (else, it will result in two voltage sources being connected in parallel).

Also, the algorithm has to ensure that the voltage applied across the load matches the load voltage just before disconnect, so that there are no inrush currents drawn by the load due to the sudden change in the load voltage.

For the transfer between the voltage-controlled mode and the current controlled mode, the inverter voltage should match the grid voltage both in magnitude and phase, before the static transfer switch can be turned on (the TRIAC should be turned on when there is essentially zero voltage across it).

Once the TRIAC is turned on, the grid current should be slowly ramped up to prevent any voltage spikes caused by the grid inductance. The proposed algorithm takes care of all the above-mentioned requirements associated with the transfer of a PWM inverter between grid-tied and off-grid modes. Moreover, the algorithm is completely independent of the actual realization of the current and voltage controllers.

### (C) Generator Control

The generator control is working in closed-loop speed control (CLSC) mode where the speed reference converter is chosen to be similar with the optimal speed in order to extract the maximum power from the wind turbine at a certain wind speed.

$$\Omega^{*} = \Omega_{opt} \qquad (6)$$

## V. GRID CONNECTED MODE TO STAND-ALONE MODE

Assume that initially the inverter is operating in the grid-tied mode. The PWM inverter is current-controlled and the grid governs the voltage at the point of common coupling (PCC). When there is a fault on the grid, the voltage at the PCC drops. The fault detection circuitry turns off the TRIAC when the grid voltage goes below a pre-set minimum value. Thus, the grid is disconnected from the inverter at the first zero crossing of the grid current, after the TRIAC has been turned off. At this instant, the PWM inverter can be shifted from current controlled mode to the voltage controlled mode.

If the load is a motor type load, or if the fault on the grid is not a dead short at the load, the voltage at the PCC will not go to zero instantaneously, but will decay exponentially. Fig. 5 shows the polar plot of the voltage for the case of a motor type load, with decaying magnitude and varying phase. In such a case, when the inverter is shifted to the voltage controlled mode, it is necessary to match the magnitude and phase of the voltage at the PCC to avoid high inrush currents. By using a DSP to monitor the voltage at the PCC, it is possible to measure the magnitude and phase of the load voltage at the instant of grid disconnect. These values form the starting magnitude and phase of the voltage reference given to the voltage controller. The voltage magnitude is then ramped up from the initial value to the rated value in the span of a couple of line cycles.

Thus the steps to be performed in the algorithm can be summarized as follows.

a) Detection of fault on the grid and give a turn off signal to the TRIAC.
b) Observe the magnitude and phase of the load voltage.
c) When the TRIAC current goes to zero, switch the inverter to a voltage-controlled mode, with the voltage reference being derived from the load voltage.
d) Ramp up the magnitude of the load voltage from its initial value to the rated value.

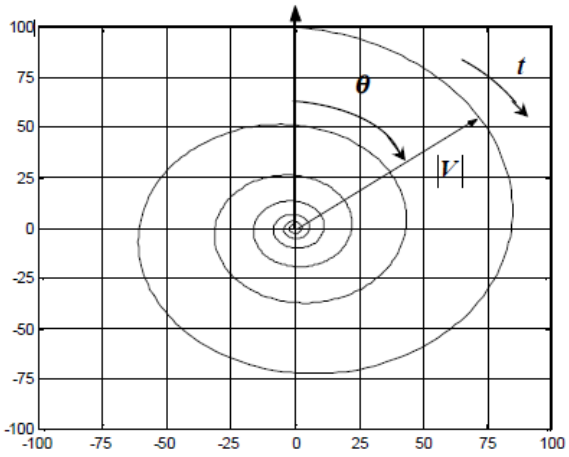


Fig. 4. Polar plot of the load voltage

## VI. STAND-ALONE MODE TO GRID-CONNECTED MODE

Assume that initially there is a fault on the grid and the inverter is operating in the voltage-controlled mode with the static transfer switch open. When the fault on the grid is cleared and the grid voltage comes back on actual value, the phase and amplitude of the load voltage (maintained by the PWM inverter) and the grid voltage may not match. Thus, before the TRIAC can be turned on to reconnect the inverter to the utility, the magnitudes and phases of the two voltages must be matched.

The magnitudes can be matched easily by ramping the inverter reference voltage up or down to match the grid voltage. However, in order to match the phase, it is necessary to increase or decrease the frequency of the load voltage until the phases match.

To determine the change in the frequency of the load voltage required to obtain a phase match in the shortest time, a simple function can be used. Fig. 5 plots the change in the load voltage frequency required ($\Delta f$) as a function of the phase of the load voltage which is measured at the rising-edge zero crossing of the grid voltage. A phase measurement of zero or $2\pi$ indicates that the two voltages are in phase. Thus at these values, the required $\Delta f$ is zero and hence the function is tapered to zero. This also ensures that once a phase match is obtained, the two voltages stay in phase. One possible problem with the function shown in Fig. 5 is the jitter which can occur if the phase is close to $\pi$. In this case, depending on the errors in measurement, $\Delta f$ will oscillate between 1 and 1, locking the two voltages out of phase permanently. This situation can be avoided by having a small hysteresis around $\pi$, as shown in Fig. 6.

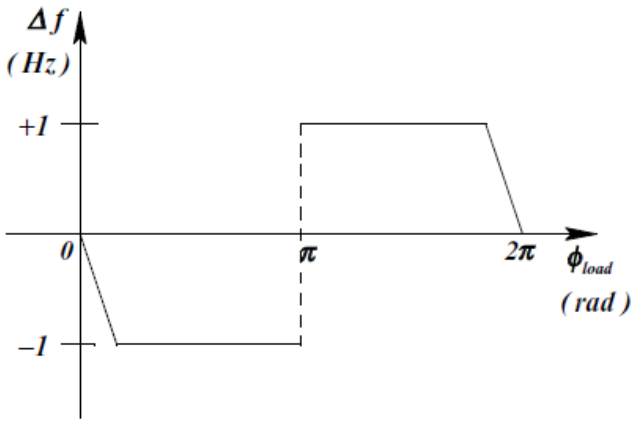


Fig. 5. $\Delta f$ as a function of $\phi_{load}$

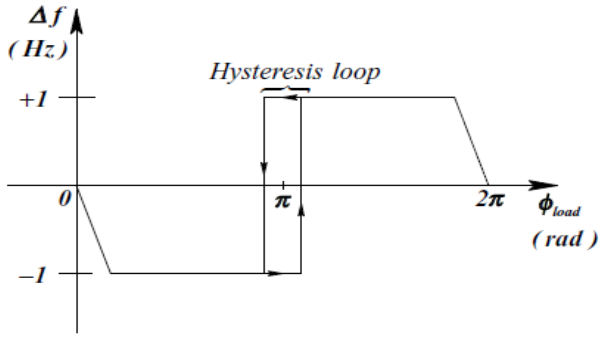


Fig. 6. $\Delta f$ as a function of $\phi_{load}$ (with hysteresis)

Once the phase and amplitude match is obtained, the PWM inverter is switched from the voltage-controlled mode to the current-controlled mode. Similar to the previous case, the current reference of the PWM inverter at the instant of turn on of the TRIAC is matched to the load current. The inverter current is then slowly changed to match the pre-specified current injection into the grid.

Thus the steps to be performed in this phase of the algorithm can be summarized as follows.

(a) Detection of the grid is within nominal operating parameters.
(b) Adjust the load voltage to match the magnitude and phase of the grid voltage.
(c) Once the load voltage is match to the grid voltage, turn on the TRIAC and switch from voltage-controlled mode to current-controlled mode, with the reference current being equal to the load current.
(d) Change the reference current slowly to the desired current (both magnitude and phase).

(i) Grid-Tied Mode to Off-Grid Mode

Figs. 7 and 8 show the simulation results for a transfer from a grid-tied mode to an off-grid mode. The grid voltage starts reducing at approximately 0.18s. Once the grid voltage reaches about 80% of its steady state value, a turn off signal is applied to the gate of the TRIAC.

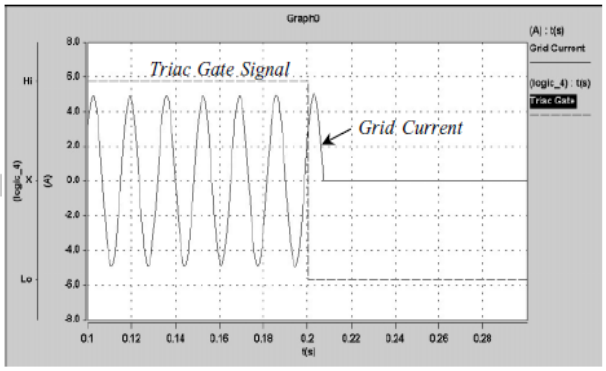


Fig. 7. Grid Current during grid-tied mode to off-grid mode transition

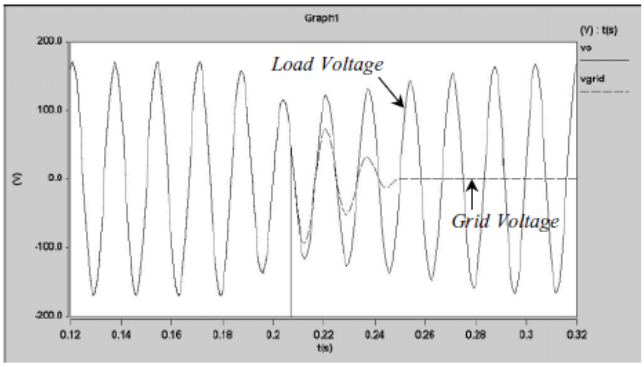


Fig. 8. Voltages during grid-tied mode to off-grid mode transition

The TRIAC turns off at the next zero crossing of the grid current (Fig. 7). We can be seen from Fig. 8, the voltage across the load is continuous at the time of disconnect from the grid, and the controller starts the inverter voltage in both amplitude and phase match with the grid. The load voltage is slowly ramped up to the rated value in about five line cycles.

Fig. 9 shows the load current, which does not have any inrush spikes during the entire transition period, indicating a smooth transition from current-controlled mode to voltage-controlled mode.

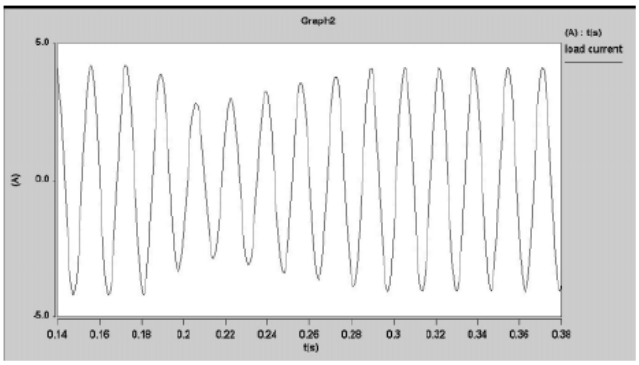


Fig. 9. Load Current during grid-tied mode to off-grid mode transition

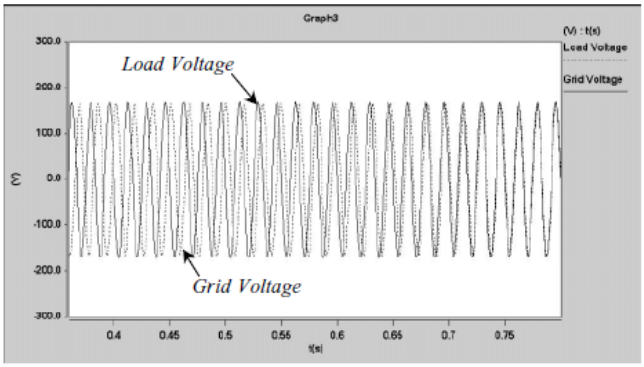


Fig. 10. Load and grid voltages during the phase-match transition

(ii) Off-Grid Mode to Grid-tied Mode

Fig. 10 shows the grid voltage and inverter output voltage during the phase match stage. The voltages start out $180^{\circ}$ out of phase and reach phase match in about 0.5sec.

Fig. 11 shows the frequency change ($\Delta f$) during this time. The value is found to start at one and gradually decrease to zero.

Fig. 12 shows the load voltage and grid current when the TRIAC is turned on. The grid current is slowly ramped up so that there are no spikes in the load voltage due to the line inductance. The load voltage is found to be smooth during the entire transition period.

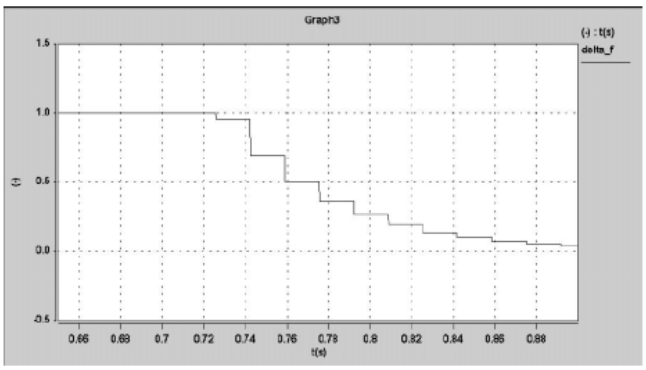


Fig. 11. Variation in $\Delta f$ with time

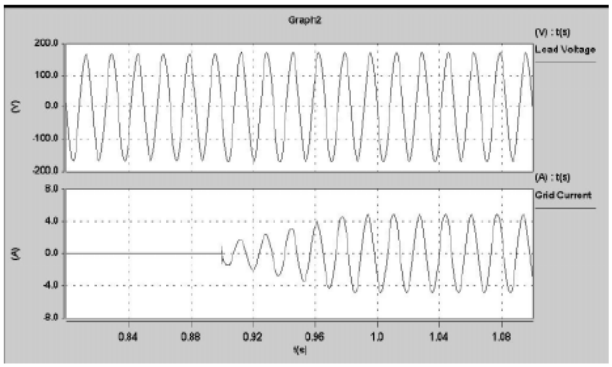


Fig. 12. Load voltage and grid current when the TRIAC is turned on

## VII. SWITCHING MODE BY PLL

Operation of small wind turbine in both Grid-Connected and Stand-Alone mode.

*Grid-Connected Control Mode:* In that grid-connected control mode, all the available power that can be extracted from the wind turbine is transferred towards the grid. Also, reactive power compensation is possible if required. The control structure for grid-connected control mode [12] is shown in Fig. 14. Standard PI-controllers are used to regulate the grid currents in the dq-synchronous frame in the inner control loops and the dc-voltage in the outer loop. A decoupling of the cross-coupling is implemented in order to compensate the couplings due to the output filter [12], [13]. The reference current in the -axis of the current loop is typically set to zero in order to get zero phase angle between voltage and current and so unity power factor can be achieved. The output of the current controllers sets the voltage reference for a standard space vector modulation (SVM) that controls the switches of the grid converter via a fiber optic link. Synchronism with grid is achieved by using a phase-locked loop (PLL). The principle of the PLL is depicted in Fig. 13. The input signals are

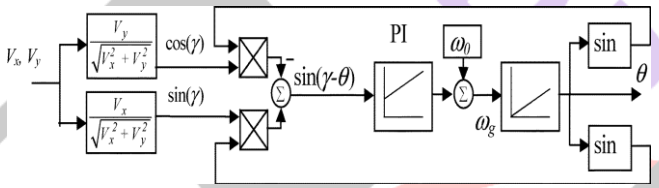


Fig. 13. PLL structure used to synchronize the inverter voltage with the grid.

$$\sin(\gamma) = \frac{V_y}{\sqrt{V_x^2 + V_y^2}}$$

$$\cos(\gamma) = \frac{V_x}{\sqrt{V_x^2 + V_y^2}} \qquad (7)$$

Where $\gamma$ is the grid phase angle, $V_x$ and $V_y$ are the grid voltage components in stationary xy-reference frame. The philosophy of the PLL is that the sinus of the difference between grid phase angle $\gamma$ and the inverter phase angle $\theta$ can be reduced to zero using a PI-controller, and thus locking the grid inverter phase to the grid, knowing that for small arguments.

$$\sin(\gamma - \theta) \cong \gamma - \theta = \Delta\theta \; V_x V_y 30^\circ \qquad (8)$$

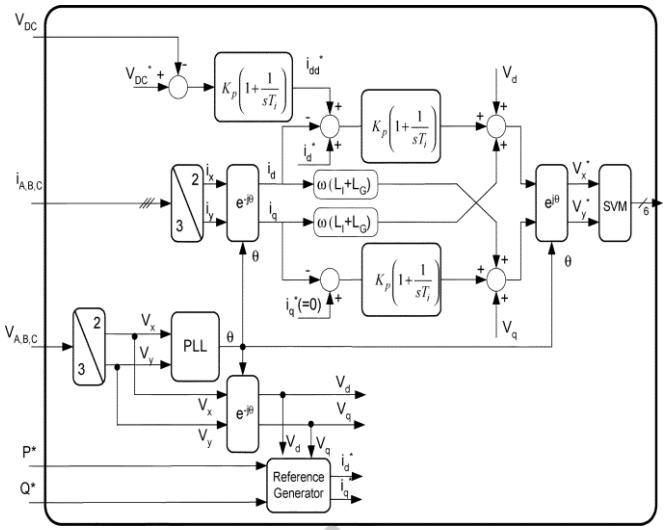


Fig. 14. Control structure for grid-connected control mode of operation.

The PLL technique including of two major parts, the phase detecting device and loop filter. The phase detecting can be readily implemented by using the dq transform in the three-phase system. The design parameters of the loop filter are the damping ratio ζ and the natural frequency ǴƆn, which determine the dynamic characteristics. The damping ratio can be selected by the Wiener method that has been generally adopted for the best optimization. The bandwidth of the loop filter is a trade-off between the filtering performance and response time. While the higher bandwidth offers the faster dynamic responses, the tracking error is increased under the distorted utility conditions. The errors caused by the phase unbalancing and harmonics have the frequency components of 2ǴƆ and multiples of 6ǴƆ, respectively, and can be considerably eliminated by using the loop filter with the low bandwidth. The error caused by the voltage offset is of the same frequency as that of the utility voltage. To reduce this error by the loop filter, the extremely low bandwidth is required. However, this degrades the dynamic performance and is not acceptable.

The presented PLL technique was lastly applied to the photovoltaic power generation system with a power rate of 10.5kW. The experimental result well demonstrated the phase tracking action of the PLL in the three-phase system.

*Stand-Alone Control Mode:* In this mode, no grid available so the output voltages need to be controlled in terms of amplitude and frequency and thus, the reactive and, resp., active power flow is controlled. In the case of unbalance between the generated and the load-required power, adjustment of the speed of the generator can regulate the produced power in a limited range.

The control structure for SA control mode is depicted in Fig. 15 and it includes of output voltage controller, dc-link voltage, damping chopper control, controller and current limiter.

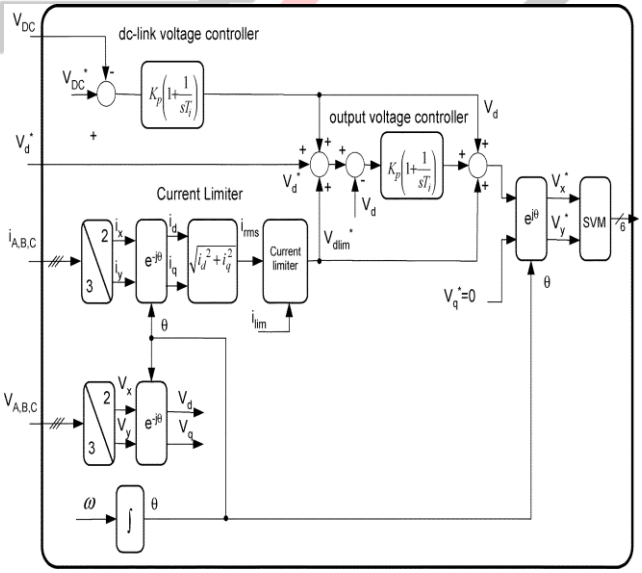


Fig. 15. Control structure for stand-alone mode of operation.

## VIII. EXPERIMENTAL RESULTS

The hardware realization of the back-to-back converter is shown in Fig. 16. As it can be observed, the system has been housed in a mobile cabinet in order to ease the field-testing.

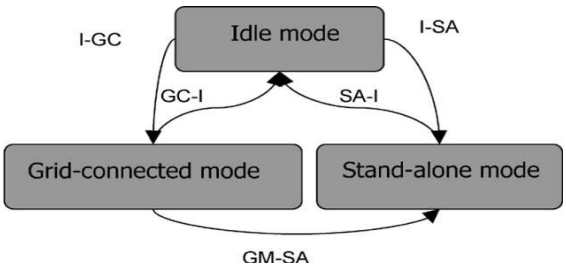


I-GC = V and /PLLe and /TRIP and START
I-SA = /V and /TRIP and START
GC-I = TRIP or STOP
SA-I = TRIP or STOP or PLLe
GC-SA = PLLe

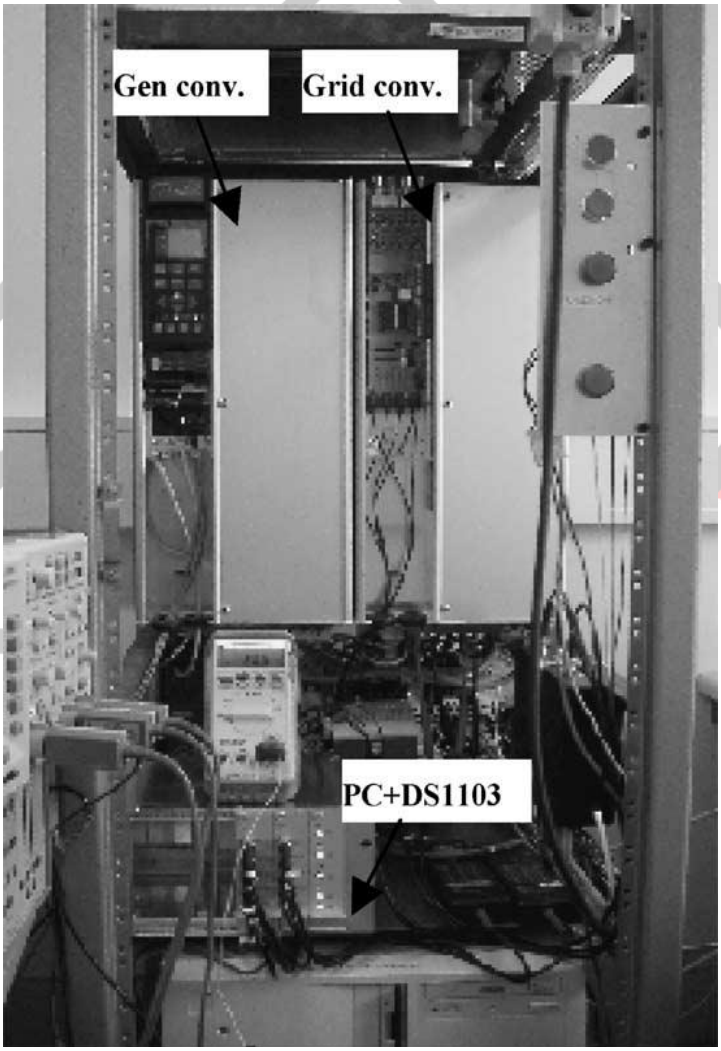


Fig. 16. B2B converter cabinet construct for the small
11-kW wind turbine test setup with dSPACE DS1103 controller.

First of all the system is tested in grid-connection mode at a 10-A step in reference of the d-current. The system response shown in Fig. 17 and demonstrates good performance of the current controller. The presence of the low-order harmonics in the current can be observed as a consequence of the grid voltage background harmonic distortion. The system is then tested in stand-alone mode generating the nominal power of 11 kW with a linear balanced resistive load. The dc-voltage was set to 620 V, and the output phase voltage was set to 230 V.

The results of experimental are shown in Fig. 18 and reveal lower harmonic distortion. The phase shift of $30^{\circ}$ between the measured voltage and current is due to the fact that the measured voltage is L-L voltage. The wind turbine is tested in stand-alone mode generating the nominal power of 11 kW with a nonlinear load created with a three-phase diode rectifier with resistive load shown in Fig. 19.

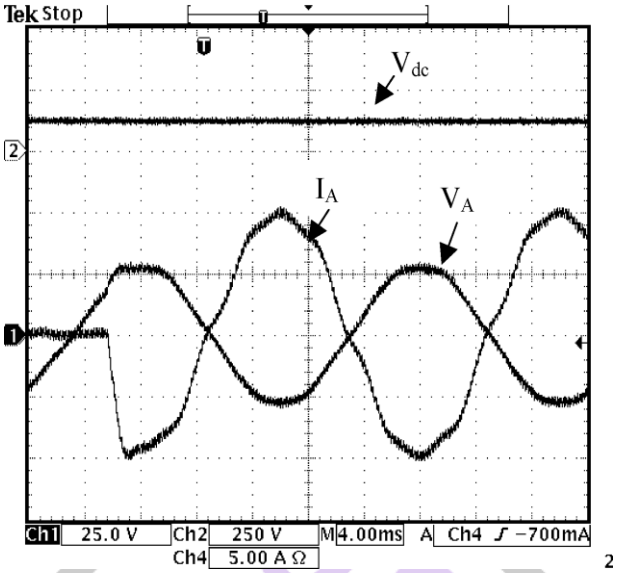


Fig. 17. Experimental test of grid-connection control mode. Current response at 10-A step in d-axis reference.

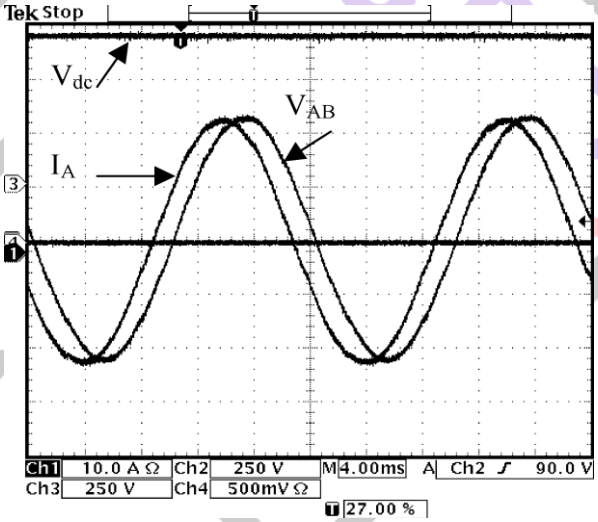


Fig. 18. Experimental test with linear load in SA mode.

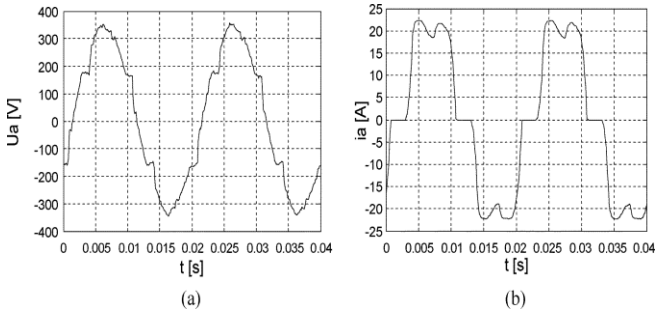


Fig. 19. Experimental test with an 11-kW nonlinear load:
(a) grid phase voltage Va and (b) grid current Ia.

## IX. CONCLUSION

This paper presents Small Wind Turbine Control with Detection of Grid Failure Operating in Both Grid and Stand-Alone system with a double B2B power converter capable of working in both mode SA as well as in grid-connection mode on a local grid. A new strategy for automatic switching between the two modes based on PLL controller is presented and successfully operated. The most useful feature of the system is the flexibility, ability to develop the control strategy. The given results show high-performance features which can be used in future wind turbine systems.

## REFERENCES

[1] A. Alesina and M. Venturini, "Intrinsic amplitude limits and optimum design of 9-switches direct PWM AC–AC converters," in *Proc. IEEE PESC'88*, 1988, pp. 1284–1291.
[2] J. Oyana, T. Higuchi, E. Yamada, and T. Lipo, "New control strategy for matrix converter," in *Proc. IEEE PESC'89*, 1989, Rec. 1989, pp. 360–367.
[3] L. Huber and D. Borojevic, "Space vector modulation with unity input power factor for forced commutated cycloconverters," in *Conf. Rec. IEEE-IAS Annu. Meeting*, 1991, pp. 1032–1041.
[4] GARDNER, R M.: 'Phaselock techniques' (John Wiley, 1979).
[5] RAZABI, B.: 'Monolithic phase-locked loop and clock recovery circuit' (IEEE Press, 1996)
[6] BLASKO, V., MOREIRA, J.C., and LIPO, T.A.: 'A new field oriented controller utilizing spatial position measurement of rotor end ring current', IEEE PESC conference record, 1989, pp. 295-299
[7] NOZARI, F., MEZS, P.A., JULIAN, A.L., SUN, *C.*, and LIPO, T.A.: 'Sensorless synchronous motor drive for use on commercial transport airplanes', *IEEE Trans.*, 1995, IA-31, (4), pp. 850-859
[8] L. H. Hansen, L. Helle, F. Blaabjerg, E. Ritchie, S. Munk-Nielsen, H. Bindner, P. Soerensen, and B. Bak-Jensen, "Conceptual survey of generators and power electronics for wind turbines," Tech. Rep. Risø-R- 1205(EN), 2001.
[9] Z. Hakan, G. Asher, J. Clare, "Dynamic Emulation of
Mechanical Loads Using a Vector-Controlled Induction Motor-Generator Set", IEEE Transaction on Industrial Electronics, Vol46, Nr. 2 April 1999.
[10] R. Cardenas, R. Peiia, G.M. Asher, J.C. Clare," Experimental emulation of wind turbines and flywheels for wind energy applications", European Power Electronics and Applications Conference, EPE200 1, Graz Austria, August 200 1, CD ROM
[11] R. Peiia, J.C. Clare, G.M. Asher, "A doubly fed induction generator using back to back PWM converters and its application to variable speed wind energy generation", IEE-Proceeding part B (Electric Power and Applications), pp. 231-241. May 1996.
[12] M. Liserre, A. Dell'Aquila, and F. Blaabjerg, "Design and control of a three-phase rectifier under nonideal operating conditions," in *Proc. IAS'02 Conf.*, vol. 2, 2002, pp. 1181–1188.
[13] M. P. Kazmierkowski, R. Krishnan, and F. Blaabjerg, *Control in Power Electronics. Selected Problems*. New York: Academic, 2002.